arXiv:1703.04621v1 [astro-ph.CO] 14 Mar 2017

Degeneracy in the spectrum and bispectrum among featured inflaton potentials

Alexander Gallego Cadavid[1,2,3], Antonio Enea Romano[1,2,3], Misao Sasaki[3]

[1]*ICRANet, Piazza della Repubblica 10,*

I–65122 Pescara, Italy

[2]*Instituto de Física,*

Universidad de Antioquia,

A.A.1226, Medellín, Colombia

[3]*Center for Graviational Physics,*

Yukawa Institute for Theoretical Physics,

Kyoto University, Japan

Abstract

We study the degeneracy of the primordial spectrum and bispectrum of the curvature perturbation in single field inflationary models with a class of features in the inflaton potential. The feature we consider is a discontinuous change in the shape of the potential and is controlled by a couple of parameters that describe the strength of the discontinuity and the change in the potential shape. This feature produces oscillations of the spectrum and bispectrum around the comoving scale $k = k_0$ that exits the horizon when the inflaton passes the discontinuity. We find that the effects on the spectrum and almost all configurations of the bispectrum including the squeezed limit depend on a single quantity which is a function of the two parameters defining the feature. This leads to a degeneracy, i.e. different features of the inflaton potential can produce the same observational effects. However, we find that the degeneracy in the bispectrum is removed at the equilateral limit around $k = k_0$. This can be used to discriminate different models which give the same spectrum.

YITP-17-25

I. INTRODUCTION

Different cosmological observations such as the Cosmic Microwave Background (CMB) anisotropies and the Large Scale Structures (LSS) have given us observational evidence that the observed universe originated from fluctuations in the very early universe [1–4]. Cosmic inflation, a period of accelerated expansion at early times, is the simplest framework able to explain the origin of these primordial fluctuations and provides a good fit to the data, while alternatives deviating from the inflationary paradigm are less compelling [1–4]. There is a plethora of inflationary models proposed in the literature which can predict the same spectrum of primordial perturbations [5–10]. In this sense deviations from Gaussian statistics of the cosmological density fluctuations, the so-called primordial non-Gaussianities (NG), are important to discriminate between different models [6–30]. Recent CMB observations [31, 32] have not completely ruled out primordial non-Gaussianity and consequently theoretical predictions could be used in the future to discriminate between different inflationary models.

Observations indicate that the spectrum of primordial curvature perturbations has some deviations from scale invariance and a possible explanation could be features of the inflaton potential [9, 17–26, 33–45] such as a step in the mass or discontinuities of other derivatives [25]. In the De Sitter limit analytical solutions for the perturbations modes can be derived and used to compute different correlation functions. Using these analytical results we show that there are classes of modified inflaton potentials which produce the same effects on the spectrum and can only be distinguished in certain limits and configurations of the bispectrum.

The paper is organized as follows. In section II we introduce the type of modifications of the inflaton potential and give analytical approximations for the background quantities. In section III we study the degeneracy of the primordial spectrum of curvature perturbations. In section IV we show how the degeneracy can be broken at the bispectrum level in certain limits and configurations of the bispectrum.

II. INFLATION AND THE MODEL

We consider a single scalar field ϕ minimally coupled to gravity according to the action

$$S = \int d^4x\sqrt{-g}\left[\frac{1}{2}M_{Pl}^2 R - \frac{1}{2}g^{\mu\nu}\partial_\mu\phi\partial_\nu\phi - V(\phi)\right], \tag{1}$$

where R is the Ricci scalar, $M_{Pl} = (8\pi G)^{-1/2}$ is the reduced Planck mass, $g_{\mu\nu}$ is the $FLRW$ metric in a flat universe, and V is the potential energy of the inflaton. The slow roll parameters

in terms of conformal time τ are defined as

$$\epsilon \equiv \frac{-H'}{aH^2} \quad , \quad \eta \equiv \frac{\epsilon'}{aH\epsilon}, \tag{2}$$

where a is the scale factor, H is the Hubble parameter, and primes indicate derivatives with respect to conformal time.

We will study the degeneracy of the spectrum and bispectrum of primordial perturbations using the following potential [24]

$$V(\phi) = \begin{cases} V_b + \frac{1}{2}m^2\phi^2, & \phi \leq \phi_0, \\ V_a + \frac{1}{2}m^2\phi^2 + \lambda\phi^n, & \phi < \phi_0, \end{cases} \tag{3}$$

where V_b and V_a are the vacuum energy before and after the feature respectively, m is the inflaton mass, λ is a parameter that controls the magnitude of the potential modification, and $\phi_0 = \phi(\tau_0)$, where τ_0 is the feature time. The condition $V_a = V_b - \lambda\phi_0^n$ ensures the continuity of the potential at ϕ_0 and the value of ϕ_0 determines the scale at which the effects of the feature appear in the spectrum and bispectrum of curvature perturbations. In the following sections we will show that the features in the spectrum and bispectrum appear around the scale $k_0 = -1/\tau_0$ which is leaving the horizon at that time.

A. Analytic approximation for the background equations

Assuming the De Sitter approximation an analytic approximation for the scalar field before and after the feature was found in [24]. Before the feature this analytic solution is

$$\phi_b(\tau) = \phi_b^+ a(\tau)^{\lambda^+}, \tag{4}$$

where ϕ_b^+ is a constant of integration, $a = (-H\tau)^{-1}$, and

$$\lambda^\pm = \frac{3}{2}\left(-1 \pm \sqrt{1 - \left(\frac{2m}{3H}\right)^2}\right). \tag{5}$$

After the feature the analytic solution is

$$\phi_a(\tau) = \phi_a^{(0)} + \phi_a^{(1)}(\tau - \tau_0) + \phi_a^{(2)}(\tau - \tau_0)^2 + \phi_a^+ a(\tau)^{\lambda^+} + \phi_a^- a(\tau)^{\lambda^-}, \tag{6}$$

where $\phi_a^{(i)} (i = 0, 1, 2)$ are constants depending on the parameters n, λ, and ϕ_0 [24]. The $\phi_a^\pm$ are constants of integration given by

$$\phi_a^\pm = \frac{\pm 1}{{a_0}^{\lambda^\pm}(\lambda^- - \lambda^+)} \left\{ \lambda^\mp \phi_0 + \phi_0' \tau_0 + \frac{n\lambda {\phi_0}^{n-2}}{m^2} \right. \tag{7}$$
$$\left. \times \left[\lambda^\mp \phi_0 + \frac{(n-1)}{(m^2 - 2H^2)} \left((m^2 + 2H^2\lambda^\mp)\phi_0' \tau_0 - \lambda^\mp H^2 \phi_0'' \tau_0^2 \right) \right] \right\},$$

where quantities evaluated at τ_0 are denoted by the subscript 0. An analytic approximation for the slow roll parameters after the feature is given by [24]

$$\epsilon_a(\tau) \approx \frac{1}{2M_{Pl}^2}\left(\lambda^+\phi_a^+ a(\tau)^{\lambda^+} + \lambda^-\phi_a^- a(\tau)^{\lambda^-}\right)^2, \tag{8}$$
$$\eta_a(\tau) \approx 2\frac{(\lambda^+)^2\phi_a^+ a(\tau)^{\lambda^+} + (\lambda^-)^2\phi_a^- a(\tau)^{\lambda^-}}{\lambda^+\phi_a^+ a(\tau)^{\lambda^+} + \lambda^-\phi_a^- a(\tau)^{\lambda^-}}.$$

III. DEGENERACY OF PRIMORDIAL SPECTRUM OF CURVATURE PERTURBATIONS

In this section we study the case in which the primordial spectrum of curvature perturbations is degenerate at all scales for different values of n and λ. We adopt the following definition for the spectrum

$$P_{\mathcal{R}_c}(k) \equiv \frac{k^3}{2\pi^2}|\mathcal{R}_c(k)|^2\,, \tag{9}$$

where k is the comoving wave number and $\mathcal{R}_c(k)$ is the Fourier transform of the curvature perturbation on comoving slices. We will consider models with the following parameters

$$m = 6.97\times10^{-9}M_{Pl}, \quad H = 3.3\times10^{-7}M_{Pl}, \quad \phi_b^+ = 10M_{Pl}, \tag{10}$$

where we can note that $m \ll H$. From now on we adopt a system of units in which $c = \hbar = M_{Pl} = 1$.

In [24] an analytic approximation for the spectrum of primordial curvature perturbations was derived for the case of the potential in eq. (3)

$$P_{\mathcal{R}_c}(k) = \frac{H^2}{8\pi^2\epsilon_a(\tau_e)}\left\{1 + \frac{D_0}{k}\left[\left(\frac{k_0^2}{k^2}-1\right)\sin\left(\frac{2k}{k_0}\right) - \frac{2k_0}{k}\cos\left(\frac{2k}{k_0}\right)\right]\right.$$
$$\left. + \frac{D_0^2}{2k^2}\left[1 + \frac{2k_0^2}{k^2} + \frac{k_0^4}{k^4} + \left(1-\frac{k_0^4}{k^4}\right)\cos\left(\frac{2k}{k_0}\right) - \frac{2k_0}{k}\left(1+\frac{k_0^2}{k^2}\right)\sin\left(\frac{2k}{k_0}\right)\right]\right\}, \tag{11}$$

where τ_e is the time at the end of inflation. The parameter D_0 is related to the discontinuity in ϕ_0'' produced by the modification of the potential. This implies that the equation for the comoving curvature perturbations

$$u_k'' + \left(k^2 - \frac{z''}{z}\right)u_k = 0, \tag{12}$$

has a Dirac delta function in z''/z, where we defined $u_k \equiv z\mathcal{R}_c(k)$ and $z \equiv a\sqrt{2\epsilon}$. To evaluate the discontinuity we integrate the Dirac delta function around the feature time [24, 46]

$$D_0 \equiv \lim_{\delta\to0}\int_{\tau_0-\delta}^{\tau_0+\delta}\frac{z''}{z}d\tau = -n\lambda a_0^2\frac{\phi_0^{n-1}}{\phi_0'} \approx n\lambda\phi_0^n\frac{3k_0}{m^2\phi_0^2}, \tag{13}$$

where we have used [24]

$$\phi_0' \approx \lambda^+ k_0 \phi_0, \quad a_0 = \frac{k_0}{H}, \text{ and } \lambda^+ \approx -\frac{1}{3}\frac{m^2}{H^2}. \tag{14}$$

In order to study the behavior of the spectrum and bispectrum we make a further approximation of eq. (7) and express it in terms of D_0 obtaining

$$\phi_a^+ \approx \phi_0\left(1 + \frac{n\lambda\phi_0^{n-2}}{m^2}\right) \approx \phi_0\left(1 + \frac{1}{3}\frac{D_0}{k_0}\right), \tag{15}$$
$$\phi_a^- \approx -\frac{\lambda^+}{\lambda^-}\frac{1}{a_0^{\lambda^-}}\frac{n\lambda\phi_0^{n-1}}{m^2} \approx -\phi_0\frac{\lambda^+}{\lambda^-}\left(\frac{H}{k_0}\right)^{\lambda^-}\frac{1}{3}\frac{D_0}{k_0},$$

where we have used eq. (14) and [24]

$$\lambda^- \approx -3\Big(1 - \frac{m^2}{9H^2}\Big), \tag{16}$$
$$\phi_0'' \approx \lambda^+ k_0^2 \phi_0 \,. \tag{17}$$

From now on we will use the new approximation in eq. (15) to derive all the analytic results below. As shown in Fig. 1 and Fig. 2 the new approximation is in good agreement with the numerical results. The above equations are crucial to understand the origin of the degeneracy of the spectrum. From eq. (8) we can in fact see that the slow roll parameters dependence on n and λ is completely determined by D_0, and for this reason the spectrum in eq. (11) is also only depending on D_0. This implies that models with the same D_0 but different n and λ will have the same spectrum, as long as

$$n\lambda\phi_0^n = \text{constant}. \tag{18}$$

In Fig. 3 we see the degeneracy of the primordial spectrum of curvature perturbations. The results of the spectrum are plotted using two different sets of values for n and λ corresponding to the same D_0. As predicted by the analytic approximation given above, models with the same D_0 have the same evolution of the primordial spectrum.

IV. BREAKING OF DEGENERACY WITH THE BISPECTRUM

As we have seen in the previous section the analytic calculations confirmed by numerical results show that a degeneracy in the spectrum of curvature perturbations is expected for models having the same D_0 parameter. In this section we will investigate if this degeneracy is also happening at the bispectrum level.

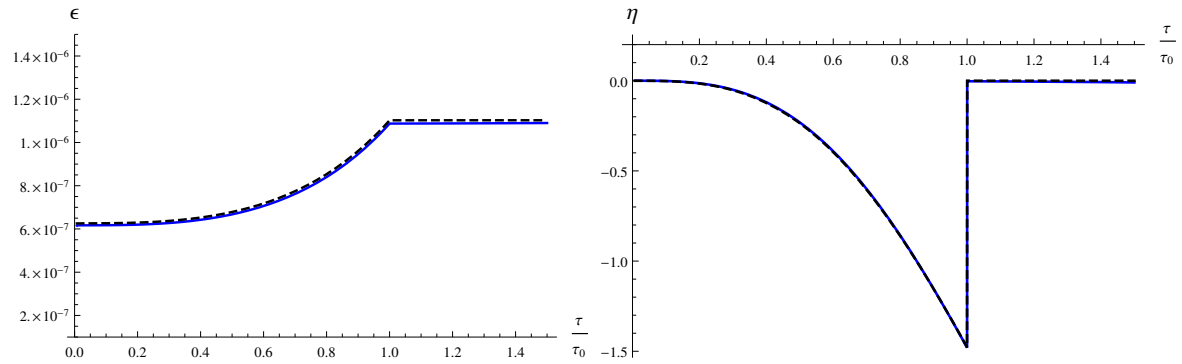

Figure 1: The numerically (blue) and analytically (black-dashed) computed slow-roll parameters are plotted for $n = 3$ and $\lambda = -4 \times 10^{-19}$. In the analytic approximation for the slow roll parametes in eq. (8) we use the approximation for $\phi_a^{\pm}$ given in eq. (15).

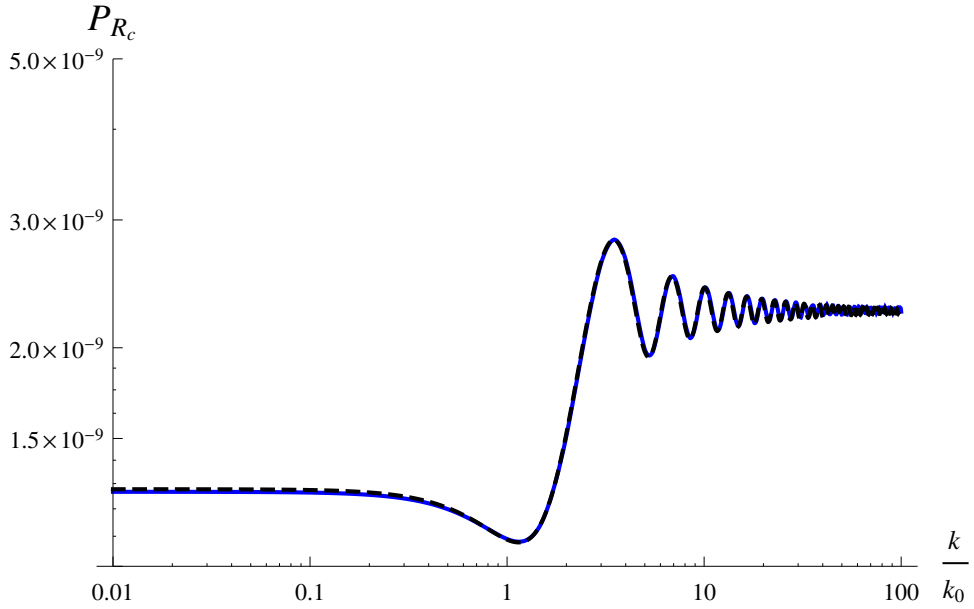

Figure 2: The numerically (blue) and analytically (black-dashed) computed spectrum of curvature perturbations is plotted for $n = 3$ and $\lambda = -4 \times 10^{-19}$. For the analytic approximation of the spectrum in eq. (11) we use the approximation for $\phi_a^{\pm}$ given in eq. (15).

A common quantity to study the non-Gaussianity is the non-linear parameter f_{NL} defined by

$$\frac{6}{5} f_{NL}(k_1, k_2, k_3) \equiv \frac{B_{\mathcal{R}_c}(k_1, k_2, k_3)}{\mathbf{P}_{\mathcal{R}_c}(k_1)\mathbf{P}_{\mathcal{R}_c}(k_2) + \mathbf{P}_{\mathcal{R}_c}(k_1)\mathbf{P}_{\mathcal{R}_c}(k_3) + \mathbf{P}_{\mathcal{R}_c}(k_2)\mathbf{P}_{\mathcal{R}_c}(k_3)}\,, \tag{19}$$

where $B_{\mathcal{R}_c}$ is the bispectrum of primordial curvature perturbations given by

$$B_{\mathcal{R}_c}(k_1, k_2, k_3) = 2\Im\Big[\mathcal{R}_c(k_1, \tau_e)\mathcal{R}_c(k_2, \tau_e)\mathcal{R}_c(k_3, \tau_e) \int_{\tau_0}^{\tau_e} d\tau \eta(\tau)\epsilon(\tau)a(\tau)^2 \tag{20}$$

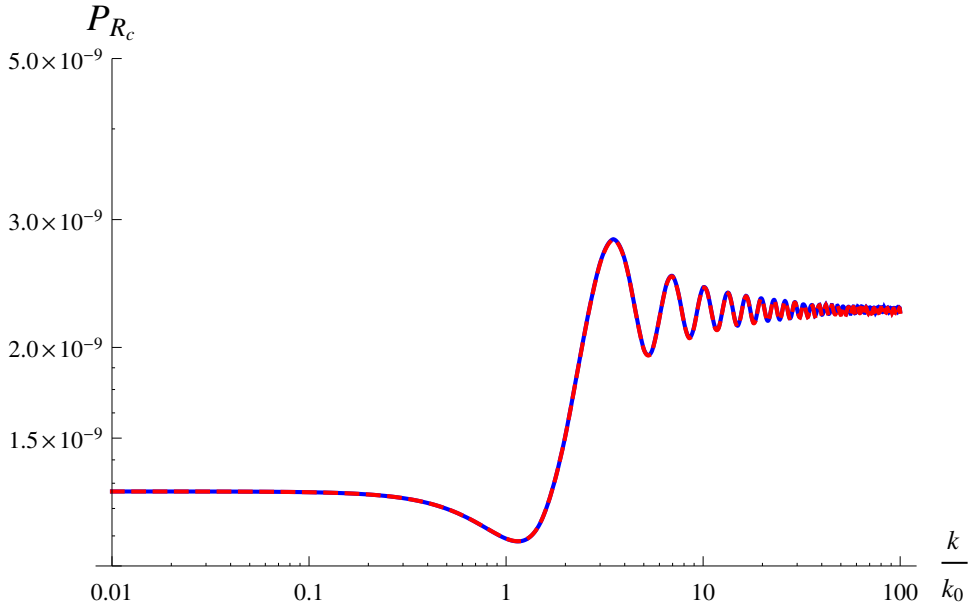

Figure 3: The numerically computed spectrum of curvature perturbations is plotted for $\{n = 3, \lambda = -4 \times 10^{-19}\}$ (blue) and $\{n = 4, \lambda = -3 \times 10^{-20}\}$ (red-dashed), corresponding to $D_0 = -0.74$. As it can be seen the spectrum is the same at all scales, as predicted by the analytical calculation.

$$\left(2\mathcal{R}_c^*(k_1,\tau)\mathcal{R}_c'^*(k_2,\tau)\mathcal{R}_c'^*(k_3,\tau) - k_1^2\mathcal{R}_c^*(k_1,\tau)\mathcal{R}_c^*(k_2,\tau)\mathcal{R}_c^*(k_3,\tau)\right) + \text{two permutations of } k_1, k_2, \text{ and } k_3\Big],$$

and

$$\mathbf{P}_{\mathcal{R}_c} \equiv \frac{2\pi^2}{k^3} P_{\mathcal{R}_c}\,. \tag{21}$$

If we replace $\mathbf{P}_{\mathcal{R}_c}$ in eq. (19) we obtain f_{NL} in terms of our definition of $P_{\mathcal{R}_c}$

$$f_{NL}(k_1,k_2,k_3) = \frac{10}{3}\frac{(k_1k_2k_3)^3}{(2\pi)^4}\frac{B_{\mathcal{R}_c}(k_1,k_2,k_3)}{P_{\mathcal{R}_c}(k_1)P_{\mathcal{R}_c}(k_2)k_3^3 + P_{\mathcal{R}_c}(k_1)P_{\mathcal{R}_c}(k_3)k_2^3 + P_{\mathcal{R}_c}(k_2)P_{\mathcal{R}_c}(k_3)k_1^3}\,. \tag{22}$$

In this paper we will use the following quantity to study the degeneracy of the primordial bispectrum [24, 25]

$$F_{NL}(k_1,k_2,k_3;k_*) \equiv \frac{10}{3(2\pi)^4}\frac{(k_1k_2k_3)^3}{k_1^3+k_2^3+k_3^3}\frac{B_{\mathcal{R}_c}(k_1,k_2,k_3)}{P^2_{\mathcal{R}_c}(k_*)}\,, \tag{23}$$

where k_* is the pivot scale at which the power spectrum is normalized, i.e., $P_{\mathcal{R}_c}(k_*) \approx 2.2\times10^{-9}$. In the equilateral limit our definition of F_{NL} reduces to f_{NL} if the spectrum is approximately scale invariant, but in general f_{NL} and F_{NL} are different. In the squeezed limit for instance they are not the same, but F_{NL} still provides useful information about the non-Gaussian behavior of $B_{\mathcal{R}_c}$ although they cannot be compared directly.

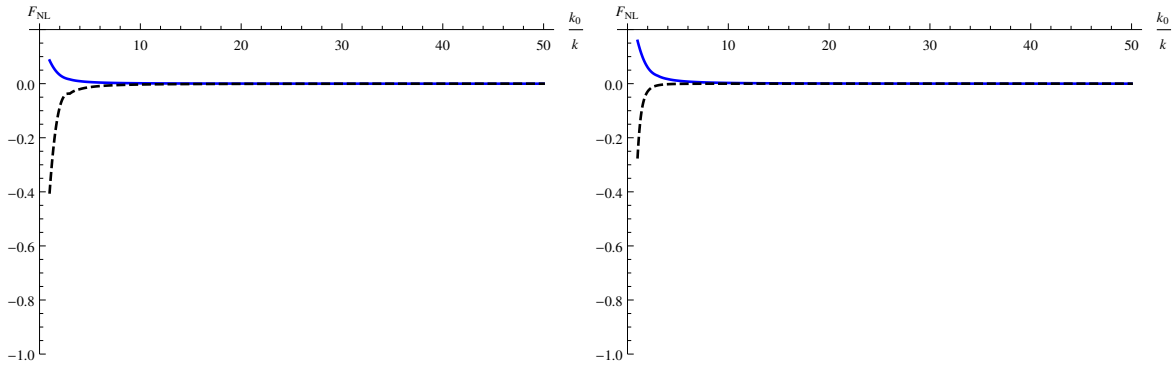

Figure 4: The numerically (blue) and analytically (black-dashed) computed large scales F_{NL} in the squeezed (left) and equilateral (right) limit is plotted for $n = 3$ and $\lambda = -4 \times 10^{-19}$.

A. Analytic approximation for the Bispectrum

Squeezed and equilateral limits at large scales

In the large scale isosceles configuration $k_2 = k_3 = k \ll k_0$ eq. (23) reduces to the following analytic formula [24]

$$F^{<}_{NL}(k_1, k) \approx -\frac{5}{6}\frac{H^5}{(2\pi)^4 P^2_{\mathcal{R}_c}(k_*)}\frac{a(\tau_e)}{(\lambda^+)^3(\phi^+_b)^6}\frac{\phi^{+2}_a}{k}\left[\frac{2k+k_1}{k_0}\cos\left(\frac{2k+k_1}{k_0}\right)\right. \\ \left. +\left(\frac{k}{k_0}\frac{2k_1+k}{k_0}-1\right)\sin\left(\frac{2k+k_1}{k_0}\right)\right]. \tag{24}$$

In the squeezed limit $k_1 \ll k$ we get

$$F^{<SL}_{NL}(k) \approx -\frac{5}{6}\frac{H^5}{(2\pi)^4 P^2_{\mathcal{R}_c}(k_*)}\frac{a(\tau_e)}{(\lambda^+)^3(\phi^+_b)^6}\frac{\phi^{+2}_a}{k}\left[\frac{2k}{k_0}\cos\left(\frac{2k}{k_0}\right)+\left(\frac{k^2}{k_0^2}-1\right)\sin\left(\frac{2k}{k_0}\right)\right], \tag{25}$$

and in the equilateral limit $k_1 = k$

$$F^{<EL}_{NL}(k) \approx -\frac{5}{6}\frac{H^5}{(2\pi)^4 P^2_{\mathcal{R}_c}(k_*)}\frac{a(\tau_e)}{(\lambda^+)^3(\phi^+_b)^6}\frac{\phi^{+2}_a}{k}\left[\frac{3k}{k_0}\cos\left(\frac{3k}{k_0}\right)+\left(\frac{3k^2}{k_0^2}-1\right)\sin\left(\frac{3k}{k_0}\right)\right]. \tag{26}$$

The results of the numerical and analytic approximation of the bispectrum are shown in Fig. 4 and are in good agreement far from k_0 both in the squeezed and equilateral limits.

Squeezed and equilateral limits at small scales

In the small scale isosceles configuration, when $k_2 = k_3 \gg k_0$ and $k_1 \gg k_0$ a fully analytic template is given by [24]

$$F^{>}_{NL}(k, k_2) \approx \frac{20}{3(2\pi)^4}\frac{(kk_2^2)^3}{(k^3+2k_2^3)P^2_{\mathcal{R}_c}(k_*)}\Im\left[\mathcal{R}_c(k,\tau_e)\mathcal{R}_c(k_2,\tau_e)^2\Big(4I_1(k_2,k,k_2)\right. \\ \left. +2I_1(k,k_2,k_2)-(k^2+2k_2^2)I_2(k,k_2,k_2)\Big)\right], \tag{27}$$

where $k = k_1 + \delta$ and δ is a phase shift parameter which varies for different models or limits, and

$$I_i(k_1, k_2, k_3) \approx \lambda^+(\lambda^-)^2\phi_a^+\phi_a^-\mathcal{A}_i(\tau_0, k_1, k_2, k_3, q_1) + (\lambda^-)^3(\phi_a^-)^2\mathcal{A}_i(\tau_0, k_1, k_2, k_3, q_2), \tag{28}$$

with $i = 1, 2$, $q_1 = 2 + \lambda^-$, and $q_2 = 2 + 2\lambda^-$. The $\mathcal{A}_i$ functions are written in the Appendix A. The analytic approximation for the curvature perturbation mode $\mathcal{R}_c$ after the feature is given by [24, 34, 47]

$$\mathcal{R}_c(k, \tau) = \frac{1}{a(\tau)\sqrt{2\epsilon_a(\tau)}}\left[\alpha_k v_k(\tau) + \beta_k v_k^*(\tau)\right] , \tag{29}$$

where

$$\alpha_k = 1 + \mathrm{i}D_0|v_k(\tau_0)|^2 \text{ and } \beta_k = -\mathrm{i}D_0 v_k(\tau_0)^2 \tag{30}$$

are the Bogoliubov coefficients and v is the Bunch-Davies vacuum.

In the small scale squeezed limit, when $k_2 = k_3 \gg k_1 > k_0$ eq. (27) reduces to

$$F_{NL}^{>SL}(k, k_2) \approx \frac{20}{3(2\pi)^4}\frac{(kk_2)^3}{P_{\mathcal{R}_c}^2(k_*)}\Im\Big[\mathcal{R}_c(k, \tau_e)\mathcal{R}_c(k_2, \tau_e)^2\Big(I_1(k, k_2, k_2) + 2I_1(k_2, k, k_2) - k_2^2 I_2(k, k_2, k_2)\Big)\Big] , \tag{31}$$

and in the equilateral limit $k_1 = k_2 = k_3 \equiv k$

$$F_{NL}^{>EL}(k) \approx \frac{20}{3(2\pi)^4}\frac{k^6}{P_{\mathcal{R}_c}^2(k_*)}\Im\Big[\mathcal{R}_c(k, \tau_e)^3\Big(2I_1(k) - k^2 I_2(k)\Big)\Big] . \tag{32}$$

The numerical results of the bispectrum and the analytic template eq. (31) and eq. (32) are in good agreement far from k_0 both in the squeezed and equilateral limits as shown in Fig. 5. In Fig. 6 we show (in the particular case of the equilateral limit) that our analytic approximation is in good agreement far from k_0 but not around the feature scale.

B. Degeneracy of the bispectrum far from k_0

The formulas in eq. (24) and eq. (27) are essential to understand the degeneracy of the bispectrum because they show that F_{NL} depends on n and λ only through the parameter $D_0(n, \lambda)$, implying a degeneracy when eq. (18) is satisfied, as long as the analytical approximation is valid.

In the large scale case it is easy to see from eq. (24) that the bispectrum depends on n and λ only through D_0 since ϕ_a^+ and $P_{\mathcal{R}_c}$ are completely determined by D_0, as we saw in previous

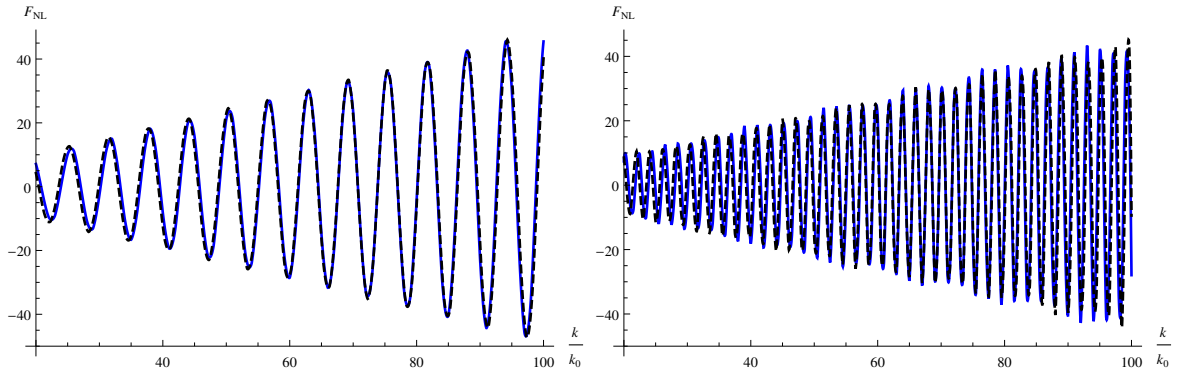

Figure 5: The numerically (blue) and analytically (black-dashed) computed small scales F_{NL} in the squeezed (left) and equilateral (right) limit is plotted for $n = 3$ and $\lambda = -4 \times 10^{-19}$. In the analytic approximation we use $\delta = 2.7k_0$ and $\delta = 0.5k_0$ in the squeezed and equilateral limits respectively.

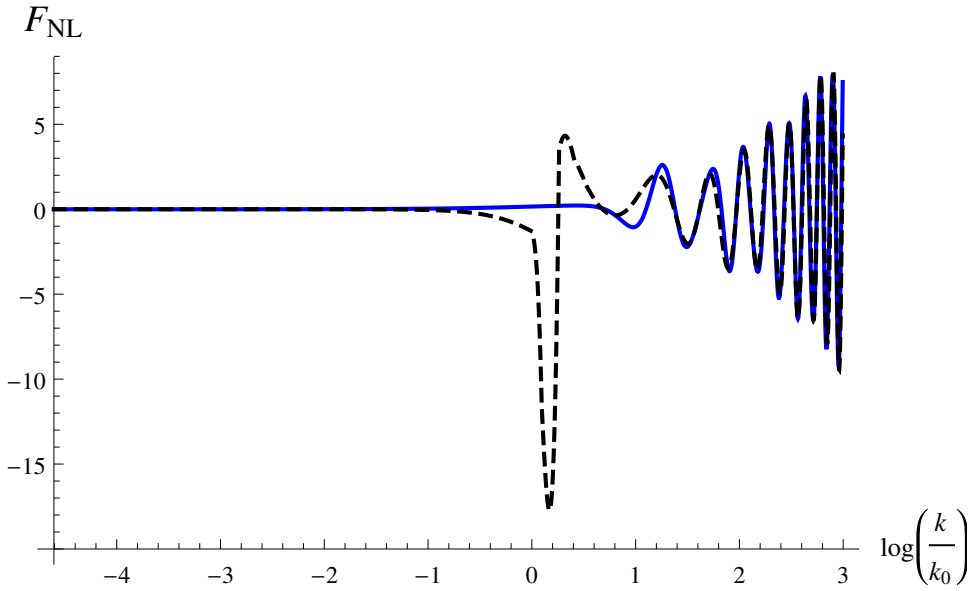

Figure 6: The numerically (blue) and analytically (black-dashed) computed F_{NL} in the equilateral limit is plotted for large and small scales around k_0 for $n = 3$ and $\lambda = -4 \times 10^{-19}$. As can be seen the analytic approximation is good for large and small scales but not around k_0.

sections. Thus the bispectrum can be degenerate at large scales in the squeezed and equilateral limits.

In the small scale case we can see from eq. (27) that the bispectrum depends on the spectrum $P_{\mathcal{R}_c}$, the curvature perturbation $\mathcal{R}_c$ after the feature, and the integrals I_i $(i = 1, 2)$. We already know that the spectrum is completely determined by D_0 while from eq. (29) and eq. (30) we can see that $\mathcal{R}_c$ depends on n and λ only through D_0. As for the integrals I_i defined in eq. (28) we can see that they depend on $\phi_a^{\pm}$ which are determined by D_0 and on the $\mathcal{A}_i$ functions

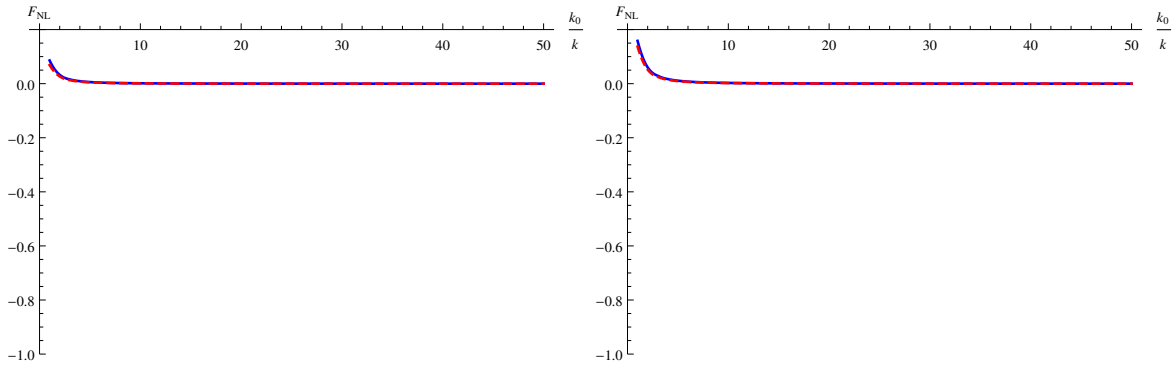

Figure 7: The numerically computed large scales F_{NL} in the squeezed (left) and equilateral (right) limit is plotted for n and λ in the case for which D_0 is the same. The parameters are $\{n = 3, \lambda = -4\times10^{-19}\}$ (blue) and $\{n = 4, \lambda = -3 \times 10^{-20}\}$ (red-dashed), corresponding to the same $D_0 = -0.74$.

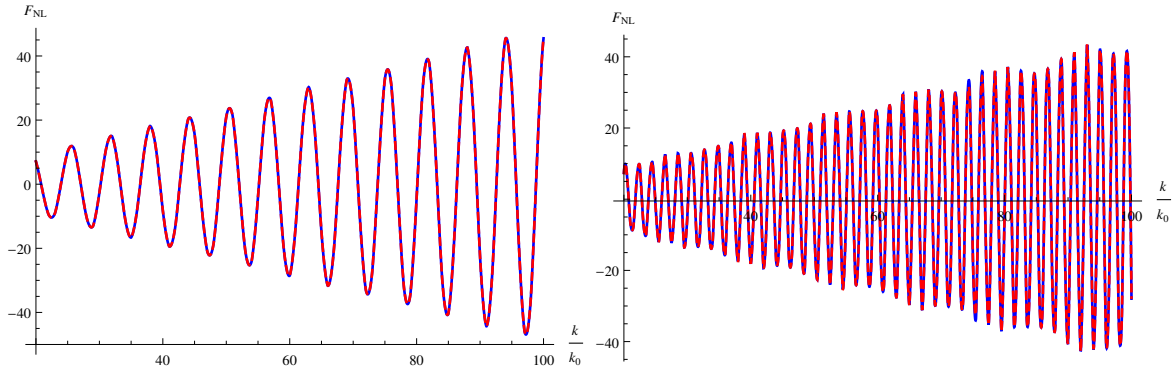

Figure 8: The numerically computed small scales F_{NL} in the squeezed (left) and equilateral (right) limit is plotted for $\{n = 3, \lambda = -4 \times 10^{-19}\}$ (blue) and $\{n = 4, \lambda = -3 \times 10^{-20}\}$ (red-dashed), corresponding to $D_0 = -0.74$.

which depend on D_0 through the Bogoliubov coefficients defined in eq. (30). Thus again the bispectrum can be degenerate at small scales in the squeezed and equilateral limits.

In Fig. 7 and Fig. 8 we show the degeneracy of the bispectrum of primordial curvature perturbations at large and small scales respectively when D_0 has the same value for different choices of n and λ. The dependence of analytical expressions for the large and small scale F_{NL} on n and λ only through D_0 explains why there is a degeneracy of the bispectrum on scales far from k_0. As shown in different figures the numerical calculations confirm the existence of this degeneracy predicted by the analytical calculations.

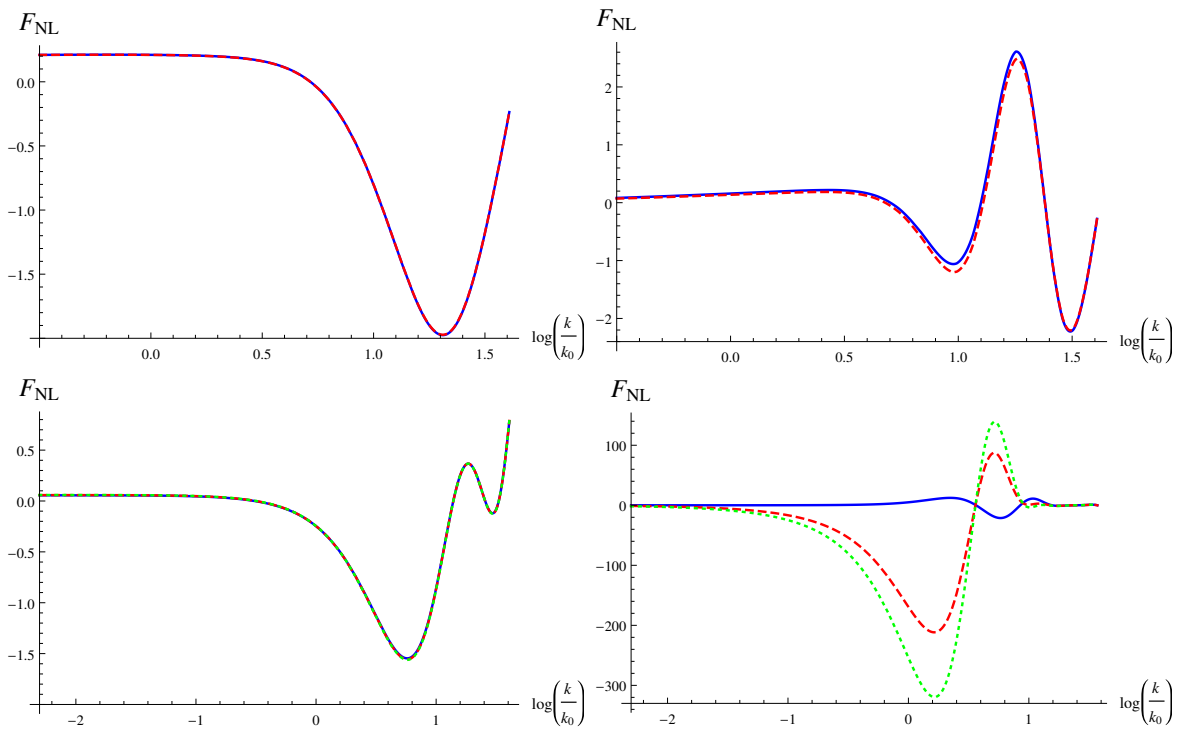

Figure 9: The numerically computed F_{NL} in the squeezed (left) and equilateral (right) limits for large and small scales around k_0 is plotted for n and λ for models that have the same D_0. On the top we have chosen $\{n = 3, \lambda = -4 \times 10^{-19}\}$ (blue) and $\{n = 4, \lambda = -3 \times 10^{-20}\}$ (red-dashed) with $D_0 = -0.74$ in both cases. On the bottom we have chosen a larger value of $D_0 = -6$ in order to see a larger breaking of the degeneracy; these values correspond to $\{n = 2/3, \lambda = -2.3 \times 10^{-15}\}$ (blue), $n = 3, \lambda = -2.4 \times 10^{-18}\}$ (red-dashed), and $\{n = 4, \lambda = -1.8 \times 10^{-19}\}$ (green-dotted).

C. Breaking of degeneracy in the equilateral limit around k_0

Around k_0 the analytical approximations used to compute the bispectrum may not be as accurate as on small and large scales, and consequently a numerical calculation is necessary. In Fig. 9 we show, for different models with the same D_0, the numerically computed bispectrum for large and small scales in the squeezed and equilateral limits. The degeneracy is broken only in the equilateral limit around k_0, while the squeezed limit is degenerate on any scale. For larger values of D_0 the breaking of the degeneracy is more evident as shown at the bottom of Fig. 9.

V. CONCLUSIONS

We have studied the degeneracy of the primordial spectrum and bispectrum of the primordial curvature perturbation in single field inflationary models with a class of features of the inflaton potential. The features consist in a discontinuous change in the shape of the potential controlled by a couple of parameters that describe the strength of the discontinuity and the change in the potential shape. The feature produces oscillations of the spectrum and bispectrum around the comoving scale $k = k_0$ that exits the horizon when the inflaton passes the discontinuity. The effects on the spectrum and almost all configurations of the bispectrum including the squeezed limit depend on a single quantity which is a function of the two parameters defining the feature. As a consequence a degeneracy is produced, i.e. different features of the inflaton potential can produce the same observational effects. The degeneracy in the bispectrum is only broken in the equilateral limit around k_0. The breaking of the degeneracy in the equilateral limit around k_0 could produce an observational signature in the CMB data which could be used to distinguish between different models predicting the same spectrum and bispectrum in other limits and configurations.

In the future it will be interesting to obtain an analytic approximation for equilateral limit bispectrum around k_0 to better understand why the degeneracy breaking only occurs in that configuration. Comparison with observations will allow to establish which modification of the inflaton potential is in better agreement with observational data. It would also be interesting to study these models within the framework of the effective theory of inflation [48] to understand if this kind of degeneracy could indeed be more general and occur for other inflationary scenarios, not only for single field minimally coupled models.

Acknowledgments

The work of A.G.C. was supported by the Colombian Department of Science, Technology, and Innovation COLCIENCIAS research Grant No. 617-2013. A.G.C. acknowledges the partial support from the International Center for Relativistic Astrophysics Network ICRANet during his stay in Italy. A.G.C. and AER thank the YITP for the kind hospitality during their visit in Kyoto. The work of M.S. was supported by the MEXT KAKENHI Grant Nos. 15H05888 and 15K21733.

Appendix A

The $\mathcal{A}_i$ functions are [24]

$$\mathcal{A}_i(\tau,k_1,k_2,k_3,q)=\frac{(-1)^i(k_2k_3)^{2(2-i)}H^{3-q}}{\left(4\epsilon_0k_1k_2k_3\right)^{3/2}}\times \tag{1}$$

$$\begin{aligned}\Big\{\alpha^*_{k_1}\Big[\quad&\alpha^*_{k_2}\Big(\mathcal{B}_i(\tau,k_1,k_2,k_3,q)\alpha^*_{k_3}-\mathcal{B}_i(\tau,k_1,k_2,-k_3,q)\beta^*_{k_3}\Big)\\ +\quad&\beta^*_{k_2}\Big(-\mathcal{B}_i(\tau,k_1,-k_2,k_3,q)\alpha^*_{k_3}+\mathcal{B}_i(\tau,k_1,-k_2,-k_3,q)\beta^*_{k_3}\Big)\Big]\\ +\beta^*_{k_1}\Big[\quad&\beta^*_{k_2}\Big(\mathcal{B}^*_i(\tau,k_1,k_2,k_3,q)\beta^*_{k_3}-\mathcal{B}^*_i(\tau,k_1,k_2,-k_3,q)\alpha^*_{k_3}\Big)\\ +\quad&\alpha^*_{k_2}\Big(-\mathcal{B}^*_i(\tau,k_1,-k_2,k_3,q)\beta^*_{k_3}+\mathcal{B}^*_i(\tau,k_1,-k_2,-k_3,q)\alpha^*_{k_3}\Big)\Big]\Big\},\end{aligned}$$

where

$$\mathcal{B}_1=(\mathrm{i}k_T)^{q-4}\Big(k_T\Gamma(3-q,-\mathrm{i}\tau k_T)+k_1\Gamma(4-q,-\mathrm{i}\tau k_T)\Big)\,, \tag{2}$$

$$\begin{aligned}\mathcal{B}_2=&(\mathrm{i}k_T)^{q-4}\Big[k_T^3\Big(\Gamma(1-q,-\mathrm{i}\tau k_T)+\Gamma(2-q,-\mathrm{i}\tau k_T)\Big)\\ &+k_T\sum_{i\neq j}^{3}k_ik_j\Gamma(3-q,-\mathrm{i}\tau k_T)+k_1\Gamma(4-q,-\mathrm{i}\tau k_T)\Big]\,,\end{aligned} \tag{3}$$

$$k_T=k_1+k_2+k_3\,,$$

and the Γ denotes the incomplete gamma functions defined by

$$\Gamma(r,x)=\int_x^\infty t^{r-1}e^{-t}dt\,. \tag{4}$$

[1] Planck, P. A. R. Ade *et al.*, Astron. Astrophys. **571**, A16 (2014), arXiv:1303.5076.

[2] Planck, P. A. R. Ade *et al.*, Astron. Astrophys. **594**, A13 (2016), arXiv:1502.01589.

[3] Planck, P. A. R. Ade *et al.*, Astron. Astrophys. **571**, A22 (2014), arXiv:1303.5082.

[4] Planck, P. A. R. Ade *et al.*, Astron. Astrophys. **594**, A20 (2016), arXiv:1502.02114.

[5] J. Martin, C. Ringeval, and V. Vennin, (2013), arXiv:1303.3787.

[6] E. Komatsu *et al.*, Non-Gaussianity as a Probe of the Physics of the Primordial Universe and the Astrophysics of the Low Redshift Universe, in *astro2010: The Astronomy and Astrophysics Decadal Survey*, , ArXiv Astrophysics e-prints Vol. 2010, 2009, arXiv:0902.4759.

[7] X. Chen, Adv.Astron. **2010**, 638979 (2010), arXiv:1002.1416.

[8] X. Chen, M.-x. Huang, S. Kachru, and G. Shiu, JCAP **0701**, 002 (2007), arXiv:hep-th/0605045.

[9] X. Chen, C. Dvorkin, Z. Huang, M. H. Namjoo, and L. Verde, JCAP **1611**, 014 (2016), arXiv:1605.09365.

[10] G. A. Palma, JCAP **1504**, 035 (2015), arXiv:1412.5615.

[11] C. T. Byrnes and E. R. M. Tarrant, JCAP **1507**, 007 (2015), arXiv:1502.07339.

[12] S. Renaux-Petel, Comptes Rendus Physique **16**, 969 (2015), arXiv:1508.06740.

[13] C. Novaes, A. Bernui, I. Ferreira, and C. Wuensche, JCAP **1401**, 018 (2014), arXiv:1312.3293.

[14] C. P. Novaes, M. Benetti, and A. Bernui, (2015), arXiv:1507.01657.

[15] E. Komatsu, Class. Quant. Grav. **27**, 124010 (2010), arXiv:1003.6097.

[16] G. Domenech, J.-O. Gong, and M. Sasaki, (2016), arXiv:1606.03343.

[17] J. Chluba, J. Hamann, and S. P. Patil, Int. J. Mod. Phys. **D24**, 1530023 (2015), arXiv:1505.01834.

[18] S. Gariazzo, L. Lopez-Honorez, and O. Mena, Phys. Rev. **D92**, 063510 (2015), arXiv:1506.05251.

[19] S. Mooij, G. A. Palma, G. Panotopoulos, and A. Soto, JCAP **1510**, 062 (2015), arXiv:1507.08481, [Erratum: JCAP1602,no.02,E01(2016)].

[20] S. Appleby, J.-O. Gong, D. K. Hazra, A. Shafieloo, and S. Sypsas, Phys. Lett. **B760**, 297 (2016), arXiv:1512.08977.

[21] P. Hunt and S. Sarkar, JCAP **1512**, 052 (2015), arXiv:1510.03338.

[22] D. K. Hazra, A. Shafieloo, G. F. Smoot, and A. A. Starobinsky, JCAP **1609**, 009 (2016), arXiv:1605.02106.

[23] S. Gariazzo, C. Giunti, and M. Laveder, JCAP **1504**, 023 (2015), arXiv:1412.7405.

[24] A. G. Cadavid and A. E. Romano, Eur. Phys. J. **C75**, 589 (2015), arXiv:1404.2985.

[25] A. G. Cadavid, A. E. Romano, and S. Gariazzo, Eur. Phys. J. **C76**, 385 (2016), arXiv:1508.05687.

[26] A. Gallego Cadavid, A. E. Romano, and S. Gariazzo, (2016), arXiv:1612.03490.

[27] Y. Xu, J. Hamann, and X. Chen, Phys. Rev. **D94**, 123518 (2016), arXiv:1607.00817.

[28] X. Chen, R. Easther, and E. A. Lim, JCAP **0706**, 023 (2007), arXiv:astro-ph/0611645.

[29] X. Chen, R. Easther, and E. A. Lim, JCAP **0804**, 010 (2008), arXiv:0801.3295.

[30] A. Gallego Cadavid, Features in single field slow-roll inflation, 2017, arXiv:1703.04375.

[31] Planck, P. A. R. Ade *et al.*, Astron. Astrophys. **571**, A24 (2014), arXiv:1303.5084.

[32] Planck, P. A. R. Ade *et al.*, Astron. Astrophys. **594**, A17 (2016), arXiv:1502.01592.

[33] S. M. Leach, M. Sasaki, D. Wands, and A. R. Liddle, Phys. Rev. **D64**, 023512 (2001), arXiv:astro-ph/0101406.

[34] A. A. Starobinsky, JETP Lett. **55**, 489 (1992).

[35] J. A. Adams, B. Cresswell, and R. Easther, Phys. Rev. **D64**, 123514 (2001), arXiv:astro-ph/0102236.

[36] A. E. Romano and P. chen, Int.J.Mod.Phys. **D20**, 2823 (2011), arXiv:1208.3911.

[37] S. Dorn, E. Ramirez, K. E. Kunze, S. Hofmann, and T. A. Ensslin, JCAP **1406**, 048 (2014), arXiv:1403.5067.

[38] G. Nicholson, C. R. Contaldi, and P. Paykari, JCAP **1001**, 016 (2010), arXiv:0909.5092.

[39] P. Hunt and S. Sarkar, JCAP **1401**, 025 (2014), arXiv:1308.2317.

[40] X. Chen, P. D. Meerburg, and M. Mnchmeyer, JCAP **1609**, 023 (2016), arXiv:1605.09364.

[41] M. Joy, A. Shafieloo, V. Sahni, and A. A. Starobinsky, JCAP **0906**, 028 (2009), arXiv:0807.3334.

[42] D. K. Hazra, M. Aich, R. K. Jain, L. Sriramkumar, and T. Souradeep, JCAP **1010**, 008 (2010), arXiv:1005.2175.

[43] M. Ballardini, F. Finelli, C. Fedeli, and L. Moscardini, JCAP **1610**, 041 (2016), arXiv:1606.03747.

[44] L. Pearce, M. Peloso, and L. Sorbo, (2017), arXiv:1702.07661.

[45] J.-O. Gong, G. A. Palma, and S. Sypsas, (2017), arXiv:1702.08756.

[46] A. E. Romano and M. Sasaki, Phys.Rev. **D78**, 103522 (2008), arXiv:0809.5142.

[47] A. A. Starobinsky, Grav.Cosmol. **4**, 88 (1998), arXiv:astro-ph/9811360.

[48] C. Cheung, P. Creminelli, A. L. Fitzpatrick, J. Kaplan, and L. Senatore, JHEP **03**, 014 (2008), arXiv:0709.0293.